Pharm Res (2013) 30:2757–2771
DOI 10.1007/s11095-013-1095-3

RESEARCH PAPER

NIR-/pH-Responsive Drug Delivery of Functionalized Single-Walled Carbon Nanotubes for Potential Application in Cancer Chemo-Photothermal Therapy

Lei Wang • Jinjin Shi • Xin Jia • Ruiyuan Liu • Honghong Wang • Zhenzhen Wang • Lulu Li • Jing Zhang • Chaofeng Zhang • Zhenzhong Zhang

Received: 16 January 2013 / Accepted: 28 May 2013 / Published online: 14 June 2013

ABSTRACT

Purpose To establish a NIR (near infrared)-/pH-responsive and sustained-release tumor-targeting drug delivery system (SWNT-PEI/DOX/NGR).

Methods Functionalized SWNTs with polymerised polymeric poly(ethylene imine) was linked NGR (Asn-Gly-Arg) tumor-targeting peptide by DSPE-PEG2000-Maleimide via the maleimide group and sulfhydryl group of cysteine, in the end, doxorubicin (DOX) was attached to SWNT-PEI to obtain a SWNT-PEI/DOX/NGR delivery system.

Results The SWNT-PEI/DOX/NGR delivery system has significantly sustained-release effect and the slow release of DOX in normal tissues contribute to reduced systemic toxicity, while under 808 nm NIR laser irradiation or under lower pH environment the release of DOX can be accelerated.

Conclusions Due to hyperthermia sensitizer effect of DOX, chemo-photothermal exemplified by SWNT-PEI/DOX/NGR tumor-targeting delivery system is a promising approach to anticancer therapy *in vivo* or *in vitro*.

KEY WORDS near infrared-responsive · pH-responsive · single-walled carbon nanotubes · sustained-release · tumor-targeting

Electronic supplementary material The online version of this article (doi:10.1007/s11095-013-1095-3) contains supplementary material, which is available to authorized users.

L. Wang • J. Shi • X. Jia • R. Liu • H. Wang • Z. Wang • L. Li • J. Zhang • C. Zhang • Z. Zhang (✉)
School of Pharmaceutical Sciences, Zhengzhou University
100 Kexue Avenue
Zhengzhou 450001, People's Republic of China
e-mail: zhangzz08@126.com

ABBREVIATIONS

DOX	doxorubicin
DPM	DSPE-PEG2000-Maleimide
NIR	near infrared
SWNT-PEI	polyethylenimine functionalized single-walled carbon nanotubes
SWNTs	single-walled carbon nanotubes

INTRODUCTION

In recent years, intelligent drug delivery systems have attracted considerable attention due to their response to external stimuli, such as temperature, pH, electric/magnetic field, light and near infrared (NIR) laser irradiation (1–4). Compared with traditional drug carriers, the intelligent drug delivery system could carry drug more effectively to the targeted tissue of complicated diseases such as cancers.

NIR-/pH-stimuli responsive carriers have been reported broadly. These two factors NIR and pH could be regulated easily by external triggers (5–7). Therefore, these NIR-responsive carriers were used in tumor local photothermal therapy due to the increasing selectivity of drugs towards tumor cells. It is known that tumor tissues have lower pH value than normal tissues (8), and doxorubicin (DOX) could be liberated rapidly in the acidic microenvironment *in vitro* and *in vivo* (9,10).

It has been proved that long-term exposure of ailing tissues to moderate drug concentrations using controlled or sustained release formulations is more beneficial than a pulsed supply of the drug at higher concentrations (11). Administration of unformulated DOX by intravenous injection leads to a spanking spiking release and a subsequent fall in the drug concentration, even below the therapeutic level in blood. Tackling this

problem head on, an effective drug carrier needs to be constructed.

As a widespread concern on nano-material carrier, SWNTs have unusual properties, resulting in being valuable for biomedical applications in a variety of areas including drug delivery, biological imaging, biosensor and photothermal therapy. However, their inherent hydrophobicity limits their application in biomedicine and thus leads to searching water-soluble SWNTs, and a lot of methods have been proposed to solve this problem (12–14). Herein, we used branched PEI to modify SWNTs.

Biological systems are known to be highly transparent under 700~1,100 nm near-infrared light. A number of studies have shown that the strong optical absorbance of SWNTs can be used for photothermal therapy (15,16). Continuous NIR irradiation can cause cell death because of excessive local heating of the SWNTs (17). And our previous study reported that the SWNT-NGR-DTX drug delivery system showed higher efficacy than docetaxel (DTX) in suppressing tumor growth *in vitro* and *in vivo* in combination with photothermal therapy (18).

In this study, we synthesised SWNT-PEI, which showed significantly sustained-release effect of DOX in normal tissues, contributing to reduced systemic toxicity. DSPE-PEG2000-Maleimide (DPM) was added to SWNT-PEI to prolong their blood circulation time and also to link NGR peptide to their surface with maleimide group to obtain a tumor-targeting drug delivery system (SWNT-PEI/DOX/NGR). NIR-/pH -responsive property of SWNT-PEI/DOX/NGR was used to improve the release of DOX at tumor region. Finally, the antitumor effect of chemotherapy-photothermal therapy of SWNT-PEI/DOX/NGR *in vitro* and *in vivo* was investigated.

MATERIALS AND METHODS

Materials

MCF-7 human breast cancer cell line (Catalog No.TCHu74) was obtained from Chinese Academy of Sciences Cell Bank. NGR peptides ($CNGRCK_2HK_3HK_{11}$) were synthesized by Shanghai Botai Biotechnology Co., Ltd. SWNTs were purchased from Chengdu Organic Chemicals Co.Ltd. (produced by CVD, purity >90%, Catalog No. 1109). Doxorubicin hydrochloride (DOX·HCl, Catalog No. D1515), DSPE-PEG2000-Maleimide (DPM, Avanti Catalog No. 880126P) and all other reagents were purchased from Sigma. Experimental animals were provided by Hunan Silaikejingda Experimental Animal Co., Ltd.

Functionalization of SWNTs with PEI

According to our previous study (19), SWNTs were suspended in 12 M HNO_3, and stirred for 24 h at room temperature to purify them. Purified SWNTs were treated with 4 M HNO_3 and 1 M HCl to obtain carboxylated SWNTs (SWNT-COOH). SWNT-NH_2 was obtained after reaction of SWNT-COOH with ethylenediamine (EDA) and dicyclohexylcarbodiimide (DCC) for 24~48 h at 120°C under reflux. After that, SWNT-NH_2 was immersed in $SOCl_2$, and then aziridine and a certain amount of HCl were added. The solution was heated to reflux for 24 h under nitrogen to obtain SWNT-PEI.

Characterizations of SWNT-PEI were investigated by transmission electron microscopy (TEM), fourier transform infrared (FT-IR) spectrum, nuclear magnetic resonance (NMR) spectrum, thermogravimetric analysis (TGA) and Water-solubility (19).

Preparation of SWNT-PEI/DOX/NGR

SWNT-PEI was put into 5 ml Milli-Q water (pH 7.4), and then 100 μl DPM (1 mg/ml) was added and was kept in ultrasonic bath for about 2 h. The supernatant was collected after centrifugation (4,000 rpm × 15 min), and NGR peptide (CNGRCK2HK3HK11, NGR: maleimide (mol/mol) = 1: 20 (20)) was added and stirred overnight at room temperature, which resulted in the production of SWNT-PEI/NGR. The solid was filtered through a membrane filter to remove excess NGR.

Thin layer silica gel chromatography using n-butanol:water:acetic acid (4:2:1) as the developing agent and 0.5% ninhydrin solution as coloring agent was used to test for conjugation of NGR to SWNT-PEI.

For preparation of SWNT-PEI/DOX/NGR and SWNT-PEI/DOX, DOX (12 mg) was added into 4 ml SWNT-PEI/NGR and SWNT-PEI (containing DPM) solution (SWNTs≈1 mg/ml) in an ultrasonic bath for about 2 h, respectively. To remove unloaded DOX, the SWNT-PEI/DOX/NGR and SWNT-PEI/DOX mixture solutions were filtered through a 0.1 μm filter with and then stored at 4°C until use.

Characterizations of SWNT-PEI/DOX/NGR

UV–Vis Spectrum

The SWNT-PEI and SWNT-PEI/DOX complexes were diluted to a certain concentration, respectively, and analyzed with an UV–vis spectrophotometer (UV-3600, Shimadzu, Japan).

Image of Transmission Electron Microscopy (TEM)

The SWNT-PEI/NGR and SWNT/DOX/NGR suspensions were dripped onto the copper line, respectively, and scanned by transmission electron microscopy (TEM, Tecnai G2 20) at 100 kV.

Drug Loading Capacity

The SWNT-PEI/DOX or SWNT-PEI/DOX/NGR resuspension was prepared as described in the section of preparation of SWNT-PEI/DOX/NGR, and the amount of DOX in delivery system was determined by an RF-5301PC spectrophotometer (Shimadzu, Japan) at ex 503 nm and em 554 nm.

The drug loading capacity was calculated by the following formulas:

$$\text{Drug loading capacity } (\%) = \frac{\text{Weight of DOX in the carrier}}{\text{Weight of carrier}} \times 100\%$$

Determination of Drug Release In Vitro

For release study, SWNT-PEI/DOX/NGR, SWNT-PEI/DOX and DOX samples were placed into dialysis tubing (Spectra/Por molecular weight cutoff 10,000), which were dialyzed in 50 ml phosphate-buffered saline (PBS, 10 mM, pH 7.4 and 5.0), respectively. The release assay was performed at 37 °C with a stirring rate of 100 rpm. 0.2 ml solution was taken from the dialysis tubing at various time points, and replaced by the same volume of fresh PBS.

For release study under 808 nm NIR laser, the treatments and groups were the same as described above with the exception that 808 nm laser irradiation was performed toward the dialysis tubing site for 1 min right after PBS replacement at each time point. The concentration of DOX released into PBS solution was quantified using HPLC under the above chromatographic conditions.

Preparation of SWNT-PEI/DOX/NGR/FITC and Cell Uptake

0.1 ml Fluorescein isothiocyanate (FITC) in dimethyl sulfoxide (1 mg/ml) was added to 5 ml SWNT-PEI/DOX/NGR, and the mixture was then sonicated and protected from light. Gel chromatography was used to remove the excess FITC by a Sephadex G-25 column (Sigma) (17).

Breast cancer cell line MCF-7 cells were cultured in normal RPMI-1640 culture medium with 10% fetal bovine serum (FBS) and 1% penicillin/streptomycin at 37°C, 5% CO_2 in an incubator (MCO-15 AC, Sanyo). The cells were plated into chambered cover-slides at a density of 1×10^5 cells/well 24 h prior to incubation with FITC, SWNT-PEI/DOX/FITC and SWNT-PEI/DOX/NGR/FITC (SWNTs was 2~5 μg/ml). The cells were incubated at 37°C for 1 h, 2 h and 4 h, respectively. After incubation, the cells were washed twice with PBS and then fixed in 4% formalin for about 15 min, and then washed with Milli-Q water to remove formalin. The cells were imaged by a fluorescence microscopy (Zeiss LSM 510).

Cell Cytotoxicity Assay

MCF-7 cells were plated in 96-well plates and incubated for 24 h. For evaluation of the cytotoxicity of SWNT-PEI/NGR on cells, MCF-7 cells were treated with various concentrations of SWNT-PEI/NGR to investigate cytotoxicity. For cell cytotoxicity measurements, DOX, SWNT-PEI/DOX, and SWNT-PEI/DOX/NGR were added to MCF-7 cells and incubated for 24 h to detect the inhibition of the cells.

For laser irradiation experiment, the cells were treated in the same way. After 4 h treatment, the cells were then subject to 808 nm NIR irradiation for 1 min. After culture for 24 h, cell viability was measured by sulforhodamine B assay (SRB).

Cell Apoptosis Detection

Changes in cell morphology were analyzed using fluorescence microscopy. The incubations of DOX, SWNT-PEI, SWNT-PEI/NGR, SWNT-PEI/DOX, SWNT-PEI/DOX/NGR (DOX: 10 μg/ml; SWNTs: ~4 μg/ml) with MCF-7 cells were carried out on cover glasses in 6-well plates. After 4 h incubation, cells were washed with PBS, and then fresh medium was added. For laser irradiation, the treatments and groups were the same as above.

After cultured for 24 h, cover glasses were fixed with methanol at −20°C for 10 min, and cells were stained with Hoechst-33258, (H-33258 10 μg/ml in distilled water for 5 min) to visualize the DNA chromatin. After being washed and air-dried, preparations were mounted in DPX (Serva, Heidelberg, Germany) and observed under UV excitation.

Xenograft Tumor Mouse Model

Female BALB/c nude mice at age of 4~6 weeks were obtained from Experimental Animal Center of Zhengzhou University, kept in filter-topped cages with standard rodent chow and water available *ad libitum*, and a 12 h light/dark cycle. The experiments were performed according to the national guidances and approved by experiment animal ethical committee. MCF-7 tumor-bearing models were established by subcutaneous injection (s.c.) of 2×10^7 MCF-7 cells in 0.2 ml PBS into the right shoulder of nude mice. The mice were used for treatment when the tumor volume reached about 100 mm^3 (7 days after tumor inoculation).

Pharmacokinetics Study

All experimental procedures were approved by experiment animal ethical committee. The saline, DOX, SWNT-PEI/DOX and SWNT-PEI/DOX/NGR were administered at a

DOX dosage of 7.5 mg/kg by tail vein injection into tumor-free healthy mice, respectively. The mice were fasted for 12 h before injection, but had access to water *ad libitum*. Blood samples were collected from the tail vein into heparinized capillaries at 0.083, 0.25, 0.5, 1, 2, 4, 8, 12 and 24 h after administration. Plasma (about 10 μl) was mixed with saline, 50% methanol, and $ZnSO_4$ (final concentration: 400 mg/ml) and centrifuged at 15,000 rpm for 10 min in a microcentrifuge; the supernatants were then collected. A 15 μl aliquot of each supernatant was mixed with 5 μl of the internal standard (daunorubicin, 10 μg/ml in methanol), 22.5 μl ice-cold methanol, and 7.5 μl Milli-Q water, and filtered through a 0.22 μm filter (Millipore).

Samples were analyzed on a Shiseido Capcell Pak C18 IF column (50×2.0 mm, 2 μm). The mobile phase consisted of a mixture of 50 mM sodium phosphate buffer (pH 2.0) and acetonitrile (65: 27, v/v). The mobile phase was delivered at a rate of 300 μl/min, and the column temperature was maintained at 25°C. The fluorescence detector was operated at an excitation wavelength of 480 nm and an emission wavelength of 550 nm.

The concentrations of DOX in plasma from the tumor-free healthy mice were measured after intravenous injection of DOX, SWNT-PEI/DOX, or SWNT-PEI/DOX/NGR. The dose of DOX used in this study was chosen to approximate the dosage of DOX used in humans.

Biodistribution Study

Animals received a single i.v. injection of free DOX, SWNT-PEI/DOX or SWNT-PEI/DOX/NGR solution at a DOX equivalent dose of 7.5 mg/kg in bacteriostatic 0.9% NaCl solution. The mice (5 per group) were sacrificed at 24 h after administration. The blood and tissues (including heart, liver, spleen, lung, kidney and tumor) were harvested, weighed and homogenized in a solution (chloroform: methanol = 4: 1) for biodistribution analyses.

In brief, tissues were homogenised into 0.2 M sodium phosphate buffer at pH 7.4, the weight ratio of tissues to buffer was 1:3. 2 ml of mixture of chloroform and methanol (4:1) was added into 200 μl homogenate or plasma and then vortexed virorously. The chloroform layers were collected after centrifugation at 4,000 rpm for 15 min at room temperature.

The concentration of DOX was determined by HPLC (1100 Agilent, USA) at the following conditions: an Agilent 1200 Eclipse XDB-C18 column (150 mm×4.6 mm, 5.0 μm); mobile phase methanol: 0.01 mol/L potassium dihydrogen phosphate: glacial acetic acid (68:31.5:0.5); column temperature 30°C; flow rate 1.0 ml/min; injection volume 40 μl; and fluorescence detection wavelength: excitation wavelength (480 nm) and emission wavelength (550 nm) (10). Absorbance at 808 nm (A808) was used to determine the SWNTs concentration in the suspension by visible spectrophotometry (UV-3600, Shimadzu, Japan) (17).

Animal Treatments

The mice were divided into six groups (5 mice per group): NS, DOX, SWNT-PEI, SWNT-PEI/NGR, SWNT-PEI/DOX or SWNT-PEI/DOX/NGR (DOX: 7.5 mg/kg, SWNTs: ~3 mg/kg) were intravenously injected into mice via tail vein every other day, respectively. The mice were observed daily for clinical symptoms and tumor sizes were measured by a caliper every other day and the volume was calculated as $(\text{tumor width})^2 \times (\text{tumor length})/2$.

After treatment for 14 days, the mice were sacrificed to collect heart, liver, spleen, lung, kidney, brain and tumor, and the collected tissues were soaked in 10% formalin solution, embedded with paraffin for H&E stain. Morphological changes were observed under Microscopy (Zeiss LSM 510).

Statistical Analysis

Quantitative data were expressed as Mean ± SD and analyzed by an analysis of variance (ANOVA) followed by Dunnett post test. P values <0.05 were considered statistically significant.

RESULTS AND DISCUSSIONS

Functionalization and Characterization of SWNT-PEI

To improve the solubility of SWNTs in water, functionalization of PEI was performed via a cationic polymerization of aziridine in the presence of amine-functionalized SWNTs (SWNT-NH_2), and SWNT-NH_2 was obtained by introducing ethylenediamine onto the surface of SWNTs. Specifically, SWNT-PEI was synthesized in this study through purification, oxidation, amination and polymerization, indicating that SWNT-PEI yield was 40±5 wt.% with great repeatability (Fig. 1).

The pristine SWNTs contained impurities such as amorphous carbons, nanoparticles, and metal catalysts. TEM results showed that the appearance of pristine SWNTs was twisted, and winded up forming a large bundle (for details see Supplementary Material Fig. S1a). However, the surface of SWNTs was significantly changed after purification (for details see Supplementary Material Fig. S1b and Fig. S1c), while SWNT-PEI (for details see Supplementary Material Fig. S1d) looked rough with a layer of material attached to the sidewalls of SWNTs.

FT-IR spectrum (for details see Supplementary Material Fig. S2a) showed no significant changes in the basic structure

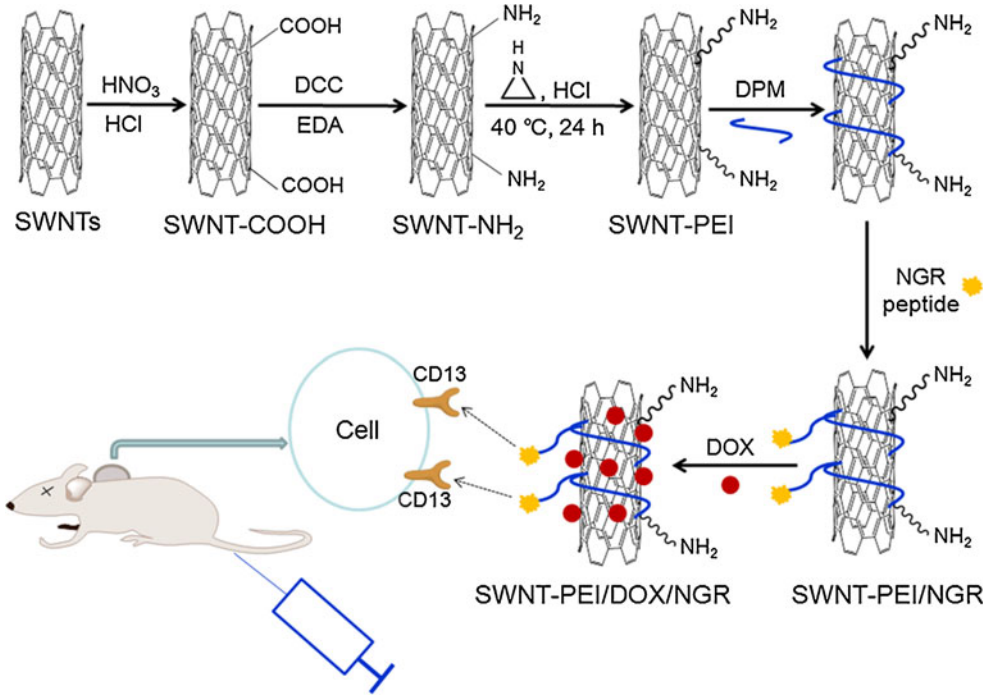

Fig. 1 The approach for preparing SWNT-PEI and SWNT-PEI/DOX/NGR drug delivery system.

of pristine SWNTs after carboxylation and amination. However, typical peaks at 1,710 cm^{-1} (Peak 1) for carboxyl group and at 1,630 cm^{-1} (Peak 2) for primary amine were found after carboxylation and amination of SWNTs, respectively. The typical peaks at 600~800 cm^{-1} (Peak 3) and 3,727 cm^{-1} (Peak 4) all indicated the attachment of amidogen to SWNTs.

Comparison of ^{1}H NMR spectrum (for details see Supplementary Material Fig. S2b) of SWNT-PEI in D_2O with that of PEI in D_2O (pH 7.0) indicated that polymerized PEI on the surface of SWNTs and pure PEI have the same chemical shift at 3.6~3.7 (ppm). The typical peak of SWNT-PEI is significantly downsized maybe due to the protonation.

The amount of PEI attached to SWNTs was investigated by thermogravimetric analysis (TGA). SWNTs were stable up to 675°C, while pure PEI was absolutely degraded at about 525°C. The weight loss of SWNTs, SWNT-NH_2 and SWNT-PEI were 0, ~1.1% and ~9.23% at 525°C, respectively, thus the weight ratio of PEI on the surface of SWNTs was ~8.12% (for details see Supplementary Material Fig. S2c).

The solubility of SWNT-COOH and SWNT-NH_2 was poor. However, SWNT-PEI showed much better solubility. Even in RPMI-1640 medium with 10% FBS SWNT-PEI was soluble and stable for weeks or even up to months (for details see Supplementary Material Fig. S2d).

Synthesis and Characterization of SWNT-PEI/DOX/NGR

To optimize drug loading time, we have detected the DOX loading capacity at 0.25 h, 0.5 h, 1 h, 2 h, 4 h, 8 h and 12 h, showing that the loading capacity of DOX reached maximum at 2 h (for details see Supplementary Material Fig. S3).

Thin layer silica gel chromatography results showed no free NGR spot after reaction with NGR peptides, indicating that NGR had been completely attached to the surface of SWNT-PEI. Maleimide in the DPM conjugate could undergo an addition reaction with the double bond in sulfhydryl groups of cysteine at room temperature to connect covalently with $CNGRCK_2HK_3HK_{11}$ (C, containing sulfhydryl groups).

The molecular basis behind NGR tumor-homing properties suggests that this motif can specifically bind to cells expressing aminopeptidase N (CD13) (21,22). Studies showed that CD13 was highly expressed in MCF-7 human breast cancer cell line, so MCF-7 cells were used in this study (23). In this study, DPM was added to reduce the toxicity of PEI induced by positive charge and conjugate NGR peptides, resulting in the biocompatibility of SWNTs and increased blood circulation time of the drug delivery system *in vivo*.

In SWNT-PEI/DOX/NGR drug delivery system (Fig. 1), DOX was adsorbed on to SWNT-PEI through π-π stacking. DOX loaded on SWNT-PEI/NGR was confirmed by a strong absorption peak at around 254 nm over SWNT-PEI/NGR background (Fig. 2a). SWNT-PEI/DOX/NGR was stable in water, cell culture medium and plasma of mice over weeks without significant aggregation (Fig. 2b).

TEM showed that some particles were attached to SWNT-PEI (Fig. 2e), demonstrating that while DOX was attached to the surface of SWNT-PEI, the surface morphology become so (Fig. 2d).

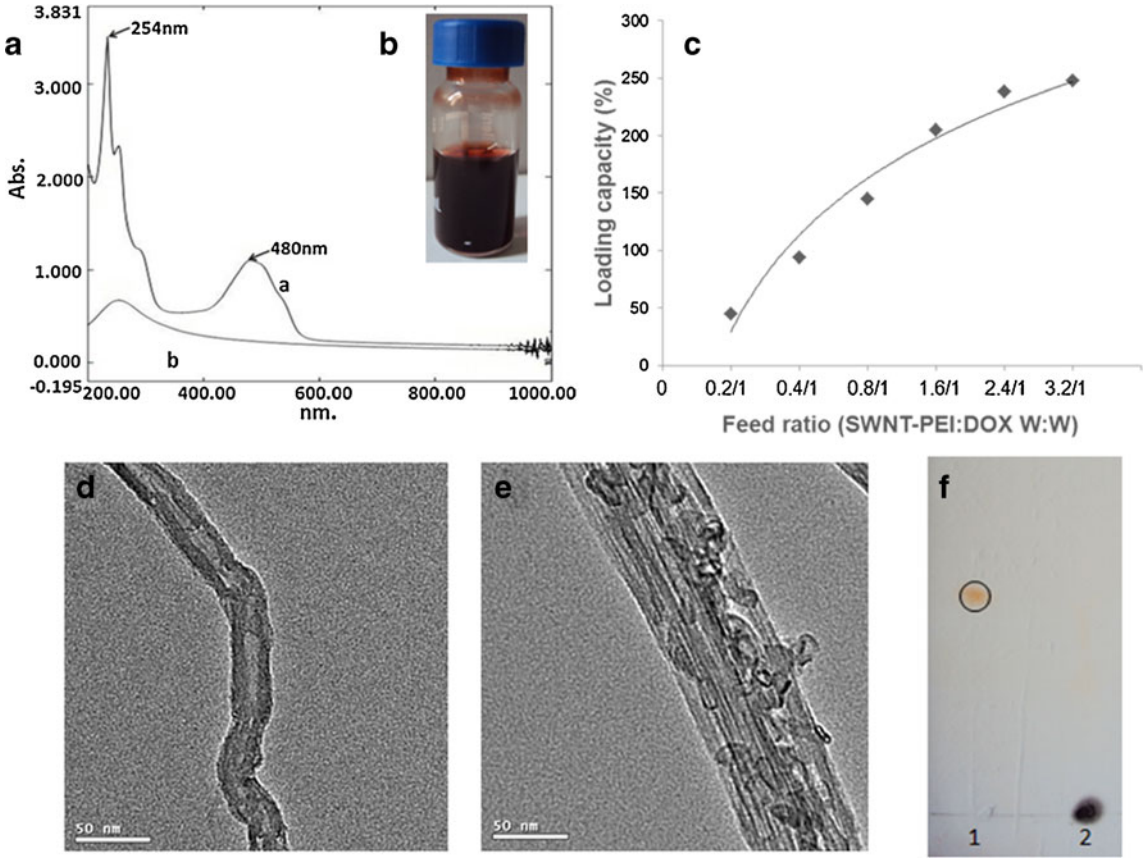

Fig. 2 **a**) UV–vis spectrum of (**a**) DOX, **b**) SWNT-PEI; (**b**) Photo of SWNT-PEI/DOX/NGR in water; (**c**) DOX loading capacity at different feeding amounts of DOX; (**d**) TEM picture of SWNT-PEI; (**e**) TEM picture of SWNT-PEI/DOX/NGR; (**f**) Thin layer silica gel chromatography image of 1-(NGR), 2-(SWNT-PEI/NGR).

To determine the capacity of DOX loading onto SWNT-PEI/NGR, different ratios of SWNT-PEI to DOX were performed. The results indicateding that DOX loading capacity increased from about 43% to 248% with increasing amount of added DOX (Fig. 2-c). A DOX loading of 248% (SWNT-PEI: DOX≈ 1: 3) was chosen for the following experiments. SWNT-PEI/DOX/NGR exhibited a high loading capacity of DOX due to the supramolecular π-π stacking between DOX and SWNT-PEI, indicating that SWNT-PEI was a promising material for drug delivery.

To investigate the release kinetics of DOX from SWNT-PEI/DOX/NGR delivery system, we incubated the delivery system in PBS (10 mM, pH 7.4 and 5.0). As shown in Fig. 3, DOX release from SWNT-PEI/NGR was sustained over 8 days. In contrast, the release of DOX group was very fast, indicating that interaction between SWNT-PEI/NGR, SWNT-PEI and DOX plays a critical role in the release of drug due to a dendritic structure of PEI grafted on the surface of SWNTs (24). It is demonstrated that the SWNT-PEI/DOX/NGR delivery system has a sustained-release manner.

Figure 3 showed the cumulative release of the DOX from the SWNT-PEI/DOX/NGR delivery system at pH 5.0 and 7.4 as a function of time. DOX release at pH 5.0 was faster than that at pH 7.4. The observed pH dependency can be attributed to increased hydrophilicity and higher solubility of DOX at lower pH caused by the protonation of -NH_2 groups, thus reducing interactions between DOX molecules and SWNTs. The microenvironments of extracellular of tumors, intracellular lysosomes and endosomes are acidic, and this

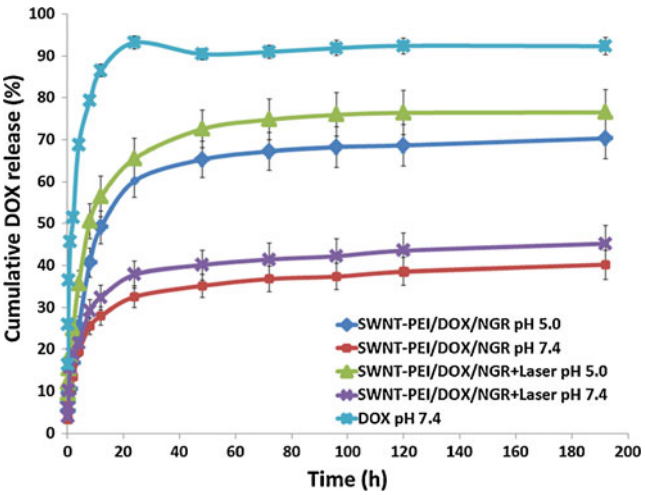

Fig. 3 DOX release profile from the SWNT-PEI/DOX/NGR at pH 5.0 and pH 7.4 with or without NIR laser irradiation. (Mean ± SD, $n = 3$).

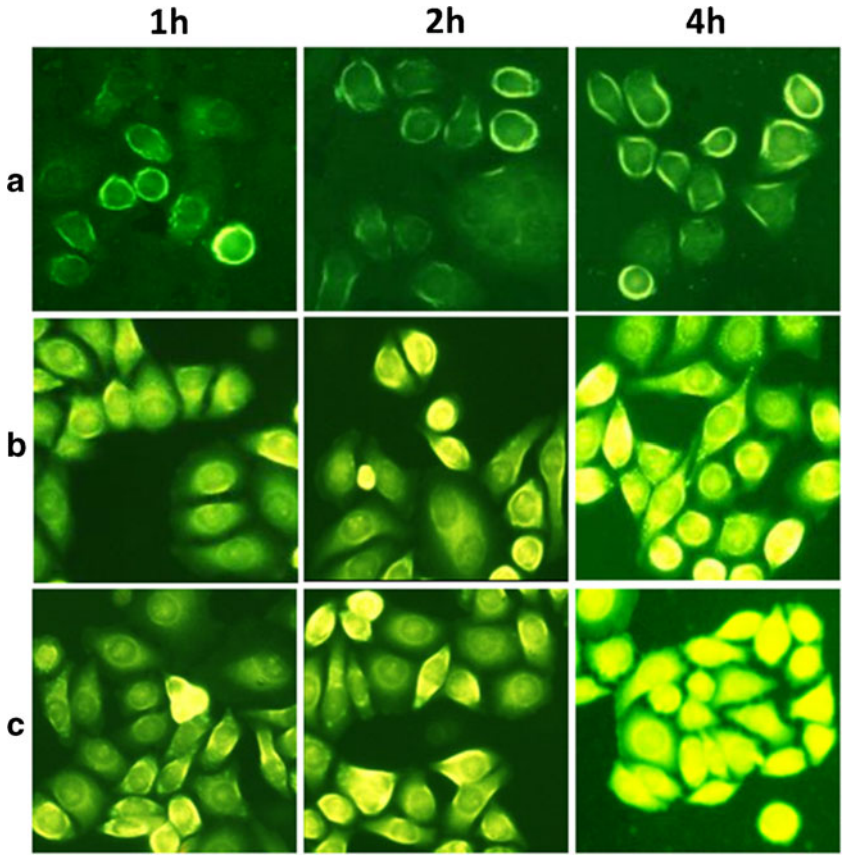

Fig. 4 Fluorescence microscopic images of MCF-7 cells: (**a**) FITC group; (**b**) SWNT-PEI/DOX/FITC; (**c**) SWNT-PEI/DOX/NGR/FITC at 1, 2, and 4 h.

acidity could facilitate DOX release from SWNT-PEI/DOX/NGR. The sustained-release and pH-responsive DOX release from SWNT-PEI/DOX/NGR could be exploited for drug delivery applications.

The DOX release *in vitro* under 808 nm NIR laser increased significantly ($P<0.05$) (Fig. 3), indicating that NIR laser not only induce heating SWNTs *in vitro* (19), but also increase the release of drugs loaded on SWNTs due to NIR-trigger (4,5) and strengthen the diffusion coefficient of the DOX molecules (25).

Cell Uptake of SWNT-PEI/DOX/NGR

As shown in Fig. 4, fluorescence microscopy was applied to track the location of the fluorescein-labeled SWNTs inside MCF-7 cells. When the cells were treated with FITC alone, FITC is mainly distributed outside the cells, suggesting little FITC in cells. However, when MCF-7 cells were incubated with SWNT-PEI/DOX/FITC and SWNT-PEI/DOX/NGR/FITC, the uptake amounts increased with time increment. Although drugs can enter cells by themselves, SWNTs still play an important role because they enable molecular targeting via the attachment of NGR peptides. Although much SWNT-PEI/DOX/NGR/FITC was taken into MCF-7 cells at 4 h, but only a part of SWNT-PEI/DOX/FITC was transferred into the cells at this time point, suggesting that NGR tumor-targeted peptide could enhance uptake of the delivery system by MCF-7 cells.

Cell Viability

The cytotoxicity study of SWNT-PEI/NGR on MCF-7 cells was carried out at different concentrations. As shown in Fig. 5a, cell inhibition remained less than 10% when the concentration of SWNTs was lower than 30 μg/ml, so the concentration of SWNTs used in the following experiments were lower than 30 μg/ml, and we consider that had no obvious toxicity to MCF-7 cells.

SWNT-PEI/NGR had no significant cytotoxicity on MCF-7 cells at the concentration of DOX of 10 μg/ml and SWNTs of about 4 μg/ml (Fig. 5a). The cell viability of DOX, SWNT/DOX, and SWNT/DOX/NGR were positively correlated with dose and time. SWNT-PEI/DOX/NGR had a higher inhibition efficiency on MCF-7 cells than SWNT-PEI/DOX and DOX alone ($P<0.05$) at 24 h (Fig. 5c); however, no significant difference between SWNT-PEI/DOX/NGR and SWNT-PEI/DOX was found at 48 h and 72 h (Fig. 5d, e), suggesting that the tumor targeting advantage of NGR is gradually reduced with prolonged time. SWNT-PEI/DOX/NGR and SWNT-PEI/DOX were both higher than DOX alone for inhibition efficiency on MCF-7

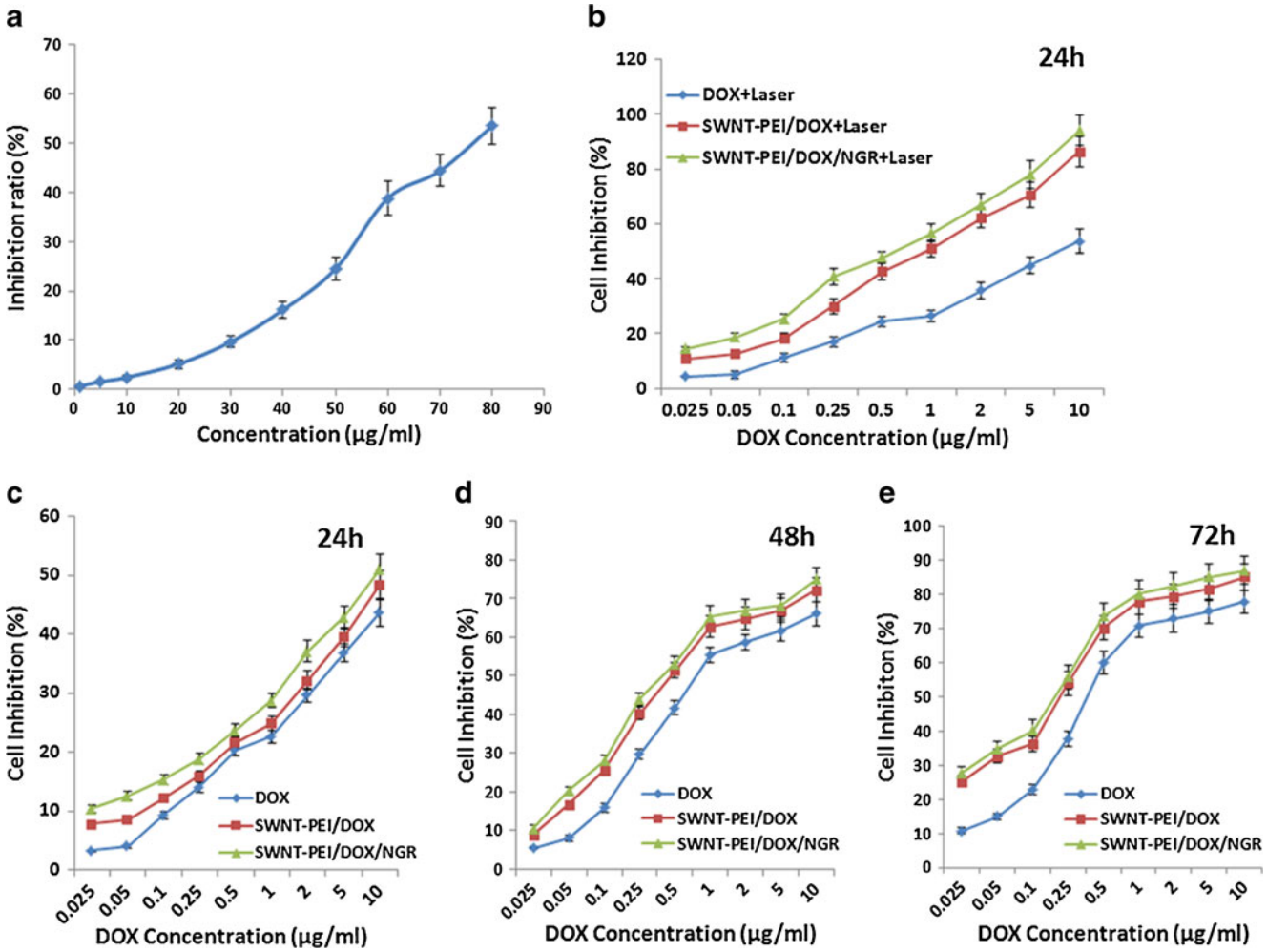

Fig. 5 (**a**) Cytotoxicity of SWNT-PEI/NGR on MCF-7 cells; (**b**) Inhibition efficiency of MCF-7 cells with NIR laser irradiation; Inhibition efficiency of MCF-7 cells at 24 h (**c**), 48 h (**d**) and 72 h (**e**). (Mean ± SD, $n = 3$).

cells ($P<0.05$) at all the time point, suggesting that the delivery system could deliver more DOX into tumor cells and enhance efficiency of inhibition on MCF-7 cells.

Compared with no laser irradiation groups (Fig. 5c), the inhibition efficiency of DOX + Laser, SWNT-PEI/DOX + Laser and SWNT-PEI/DOX/NGR + Laser groups on MCF-7 cells were all increased ($P<0.05$), respectively (Fig. 5b). As shown in Fig. 5b, the inhibition efficiency of SWNT-PEI/DOX/NGR + Laser group were significantly increased compared with control groups. Due to excessive local heating, functionalized SWNTs can be used for photothermal therapy under NIR laser (15,26,27). Kosuge *et al.* reported that photothermal destruction of macrophage cells (RAW264.7) were performed with SWNTs exposed to an 808-nm light source (28). Zhou *et al.* used FA-SWNT effectively enhance the photothermal destruction on tumor cells (15). And the results in this study were agreement with the above reports, hypothesized that heat produced by SWNTs killed cancer cells, and DOX is a temperature- and pH-responsive drug (7,29) to suppress cell growth more effectively at higher temperature (with NIR laser treatment) and at lower pH value (the microenvironments of extracellular of tumor cells). In addition, NIR laser can trigger drug release (30). Sherlock *et al.* (31) reported that highly efficient loading of DOX by π-stacking on the graphitic shell to afford FeCo/GC-DOX complexes and pH sensitive DOX release from the particles. They observed enhanced intracellular drug delivery by FeCo/GC-DOX under NIR laser (808 nm) inducing hyperthermia, resulting in a significant increase of FeCo/GC-DOX toxicity toward breast cancer cells. Due to the above reasons, the SWNT-PEI/DOX/NGR delivery system was exhibited significantly antitumor effect on MCF-7 cells with 808 nm NIR laser treatment.

Cell Apoptosis

With H-33258 stained, characteristic morphological changes of MCF-7 cells were found in fluorescence photomicrographs (Fig. 6). It was found that apoptosis rate of control

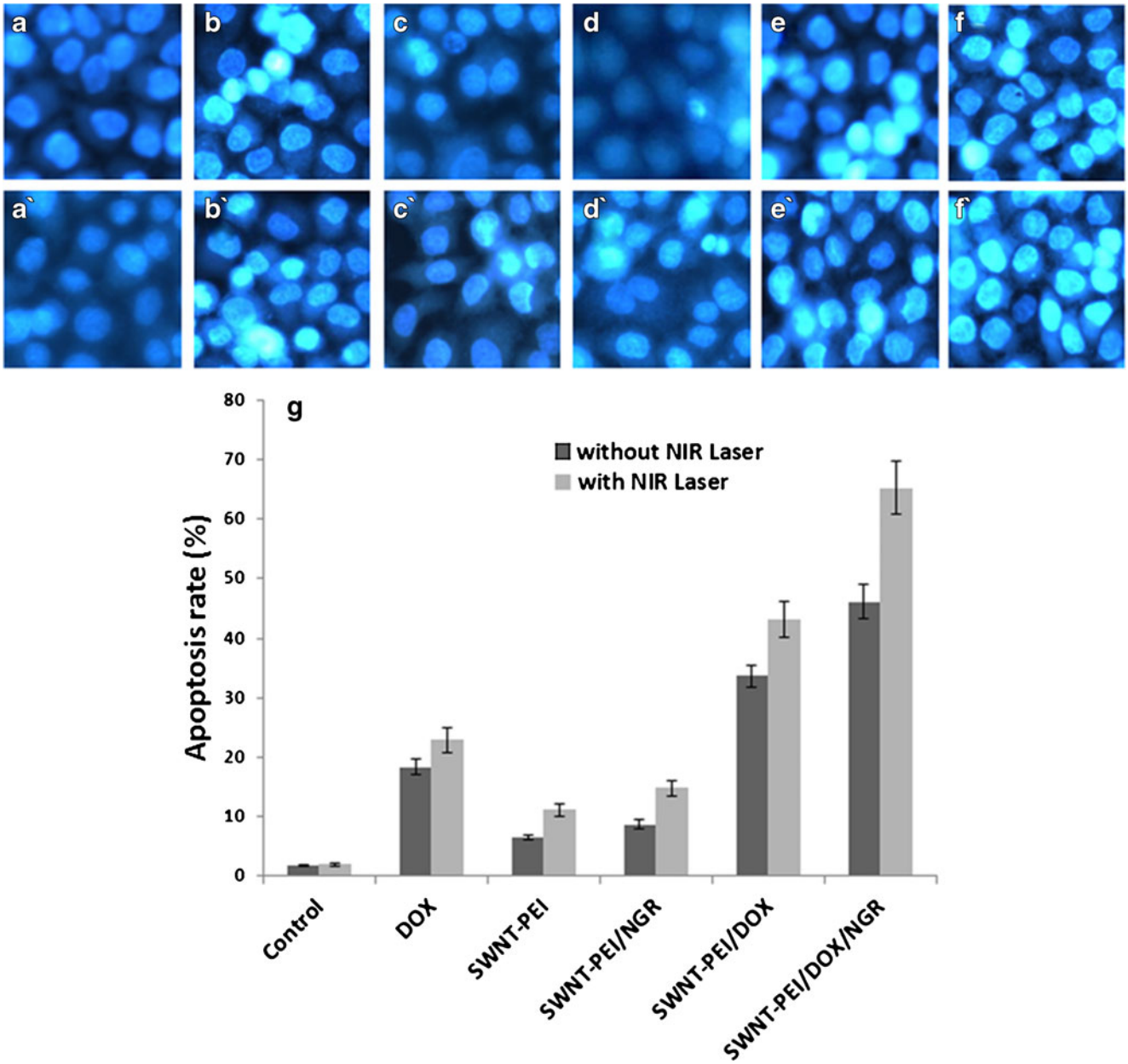

Fig. 6 Fluorescence photomicrographs of MCF-7 cells with (A', B', C', D', E', F') or without (**a**, **b**, **c**, **d**, **e**, **f**) NIR laser treatment: the groups from left to right were Control, DOX, SWNT-PEI, SWNT-PEI/NGR, SWNT-PEI/DOX and SWNT-PEI/DOX/NGR group (200×). (**g**) Apoptosis rate of MCF-7 cells with or without NIR laser irradiation. (Mean ± SD, $n = 200$).

group was about 1.8±0.23%, and there is no significant difference between control group and control + Laser group 2.0±0.25% (Fig. 6).

However, DOX, SWNT-PEI, SWNT-PEI/NGR and SWNT-PEI/DOX/NGR caused significant apoptosis in MCF-7 cells with an apoptotic rate of 18.4±1.58%, 6.5±0.43%, 8.7±0.51% and 38.6±2.45%, respectively, compared with control group ($P<0.05$), demonstrating that DOX and SWNT-PEI/NGR could induce apoptosis, separately, while the apoptosis cells rate of SWNT-PEI/DOX/NGR was significantly higher than other groups ($P<0.05$), respectively. With NIR laser irradiation, the amount of apoptotic cells increased obviously with the exception of control group. DOX, SWNT-PEI, SWNT-PEI/NGR, and SWNT-PEI/DOX/NGR could induce cell apoptosis, and the apoptotic rate increased significantly under 808 nm laser treatment, respectively ($P<0.05$), indicating that there was an synergistic effect while the cells were treated with SWNT-PEI/DOX/NGR delivery system under NIR laser.

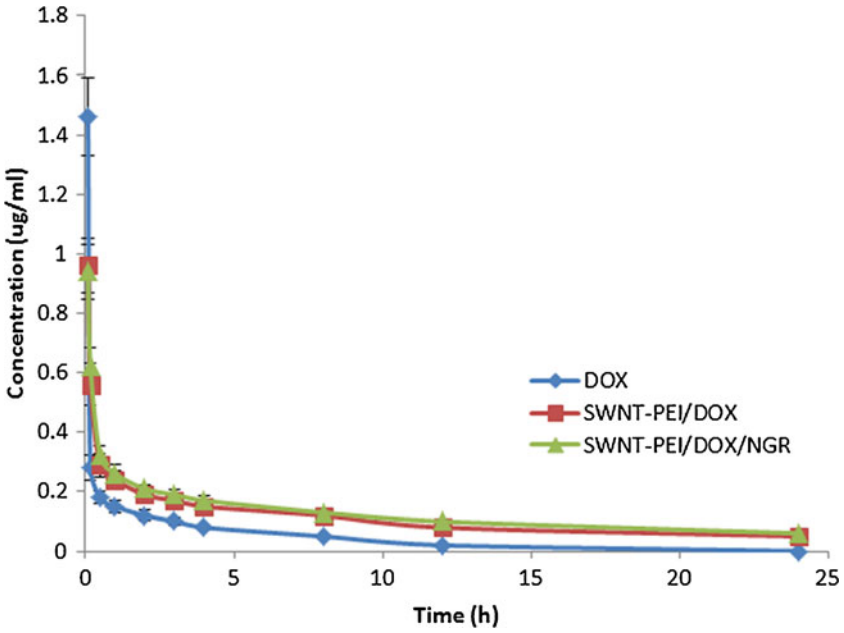

Fig. 7 Mean DOX concentration in plasma after intravenous administration of DOX, SWNT-PEI/DOX, and SWNT-PEI/DOX/NGR (Mean ± SD, $n = 5$).

Pharmacokinetics and Biodistribution

To investigate the pharmacokinetics of this delivery system, we determined DOX concentration by HPLC in blood samples of BALB/c mice after injection of DOX, SWNT-PEI/DOX, or SWNT-PEI/DOX/NGR at different times (Fig. 7). These results suggested the rate of decrease of DOX was faster than that of SWNT-PEI/DOX and SWNT-PEI/DOX/NGR after administration. The DOX concentration in blood declined below the quantitation limit, while the decrease rate of SWNT-PEI/DOX and SWNT-PEI/DOX/NGR was evidently slower, and the decrease rates in between these two groups were not significantly different, but both were markedly different from that of the DOX group ($P<0.05$).

The area under the curve ($AUC_{0\text{-inf}}$) and the area under the first moment of the plasma concentration-time curve (AUMC) of SWNT-PEI/DOX/NGR (4.096 (μg/ml)*h and 70.712 μg/ml*h^2) was about 3 times and 15 times greater than that of DOX (1.472 (μg/ml)*h and 4.789 μg/ml*h^2), respectively. The elimination rate (CL) of SWNT-PEI/DOX/NGR and DOX were 1.831 and 5.095 ((mg/kg)/(μg/ml)/h) (Table I). The mean residence time (MRT) of SWNT-PEI/DOX/NGR (17.265 h) was about 5 times longer than that of DOX (3.254 h), indicating that SWNT-PEI/DOX/NGR significantly improved the blood circulation time of DOX *in vivo* and this tumor-targeting drug delivery system has a role in sustained-release of DOX, which is consistent with the results *in vitro*.

The biodistribution of DOX, SWNT-PEI/DOX and SWNT-PEI/DOX/NGR was investigated to understand the tumor treatment efficacy of various DOX formulations. As shown in Fig. 8, there were significant differences for the biodistributions of DOX in the three formulations. Differences in biodistributions of DOX were obvious at 4 h after injection, and SWNT-PEI/DOX with high DOX concentrations in liver, spleen and lung were observed.

Table I The pharmacokinetic parameters of DOX after intravenous administration of DOX, SWNT-PEI/DOX, and SWNT-PEI/DOX/NGR in mice, respectively. ($n = 5$)

Parameter	Unit	DOX	SWNT-PEI/DOX	SWNT-PEI/DOX/NGR
$t_{1/2\alpha}$	h	0.023	0.06	0.079
$t_{1/2\beta}$	h	3.495	0.748	0.872
$t_{1/2\gamma}$	h	–	11.434	13.006
V	(mg/kg)/(μg/ml)	0.463	3.785	4.726
CL	(mg/kg)/(μg/ml)/h	5.095	2.202	1.831
$AUC_{0\text{-t}}$	μg/ml*h	1.384	2.685	3.051
$AUC_{0\text{-inf}}$	μg/ml*h	1.472	3.406	4.096
AUMC	μg/ml*h ^ 2	4.789	51.172	70.712
MRT	h	3.254	15.022	17.265

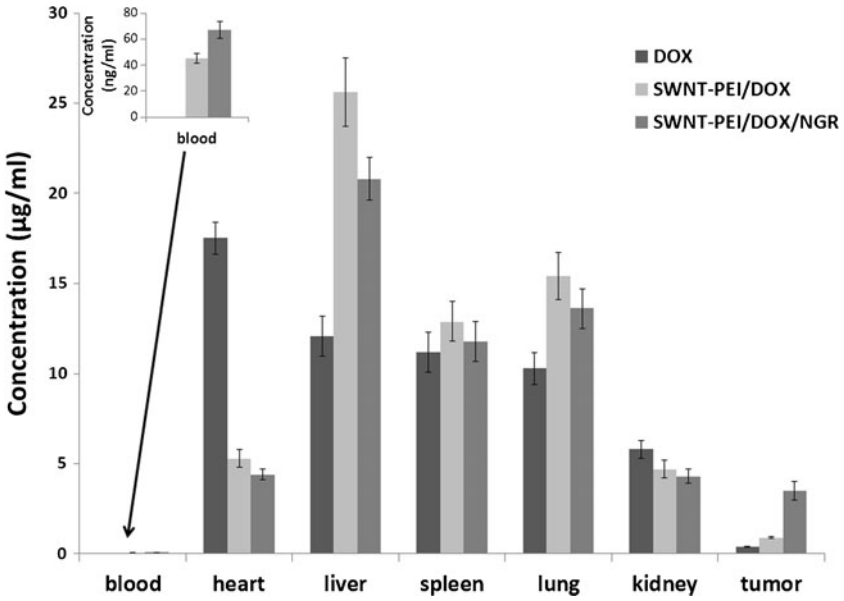

Fig. 8 Biodistribution in MCF-7 tumor-bearing nude mice injected with DOX, SWNT-PEI/DOX, and SWNT-PEI/DOX/NGR at 4 h after injection (i.v.). (Mean ± SD, $n = 5$).

Compared with DOX group, the concentrations of DOX in heart were both significantly lower than the other two groups, respectively. It is known that DOX has distinct cardiac toxicity, however, the DOX delivery system in the study can decrease the DOX concentration in heart, suggesting that it can reduce cardiac toxicity. The value of DOX of the SWNT-PEI/DOX and SWNT-PEI/DOX/NGR groups were much lower in blood at 24 h after injection, while the DOX alone group can not be detected (Fig. 8, inset).

It is worth noting that the tumor uptake of DOX in SWNT-PEI/DOX/NGR group was significantly higher than that in SWNT-PEI/DOX group and DOX group ($P<0.05$). The higher drug delivery efficiency to tumor by SWNT-PEI/DOX/NGR was striking and directly responsible for its higher tumor suppression efficacy than the other formulations.

Tumor Growth Inhibition of Tumor *In Vivo*

The treatments were done by injection of DOX, SWNT-PEI, SWNT-PEI/NGR, SWNT-PEI/DOX and SWNT-PEI/DOX/NGR (DOX dose: 7.5 mg/kg, SWNT dose: 3- mg/kg, once every 2 days) i.v. into MCF-7 tumor-bearing nude mice. As shown in (Fig. 9b), time-related changes in tumor volume were observed in all groups. After 14 days treatment, compared with the saline (NS), apparently decreased in tumor size was found in SWNT-PEI/DOX and SWNT-PEI/DOX/NGR groups, respectively ($P<0.05$), While the SWNT-PEI/DOX/NGR has a significant difference compared with the SWNT-PEI/DOX group ($P<0.05$). The *in vitro* release result showed that lower pH value can reduce interactions between DOX molecules and SWNTs to increase the release rate of DOX in tumor region. While there was no significant difference observed among the three groups of NS, SWNT-PEI and SWNT-PEI/NGR, suggesting that the reduction in tumor size was related to DOX treatment.

The tumor size in the SWNT-PEI and SWNT-PEI/NGR groups with laser irradiation were decreased compared to SWNT-PEI ($P<0.05$) and SWNT-PEI/NGR ($P<0.05$) groups without laser irradiation, respectively. No significant difference was found between the NS group and NS + laser group (Fig. 9a), suggesting that laser irradiation did cause tumor growth inhibition through SWNTs.

It was found that there was a significantly smaller tumor volume in the SWNT-PEI/NGR + laser ($P<0.05$) and SWNT-PEI/DOX/NGR + laser group ($P<0.05$) compared with the SWNT-PEI + laser and SWNT-PEI/DOX + laser group, respectively, suggesting that NGR peptide mediated more SWNTs to be transferred into tumors, consequently inducing more effective hyperthermia.

Consequently, the SWNT-PEI/DOX/NGR + laser group showed the strongest antitumor effect, which confirmed that radiation at 808 nm can significantly enhance the antitumor effect. This strongest antitumor effect resulted not only from the photothermal therapy effect of SWNTs (32,33), but also from the NIR-/pH-responsive drug release effect (25,34) and the NGR tumor targeted effect (22,35). Allowing for high toxicity usually leads to weight loss (36,37), we measured the body weight of MCF-7 tumor-bearing nude mice during the treatments, and no weight loss was observed (Fig. 9e, f), indicating that there was no significant cytotoxicity of this drug

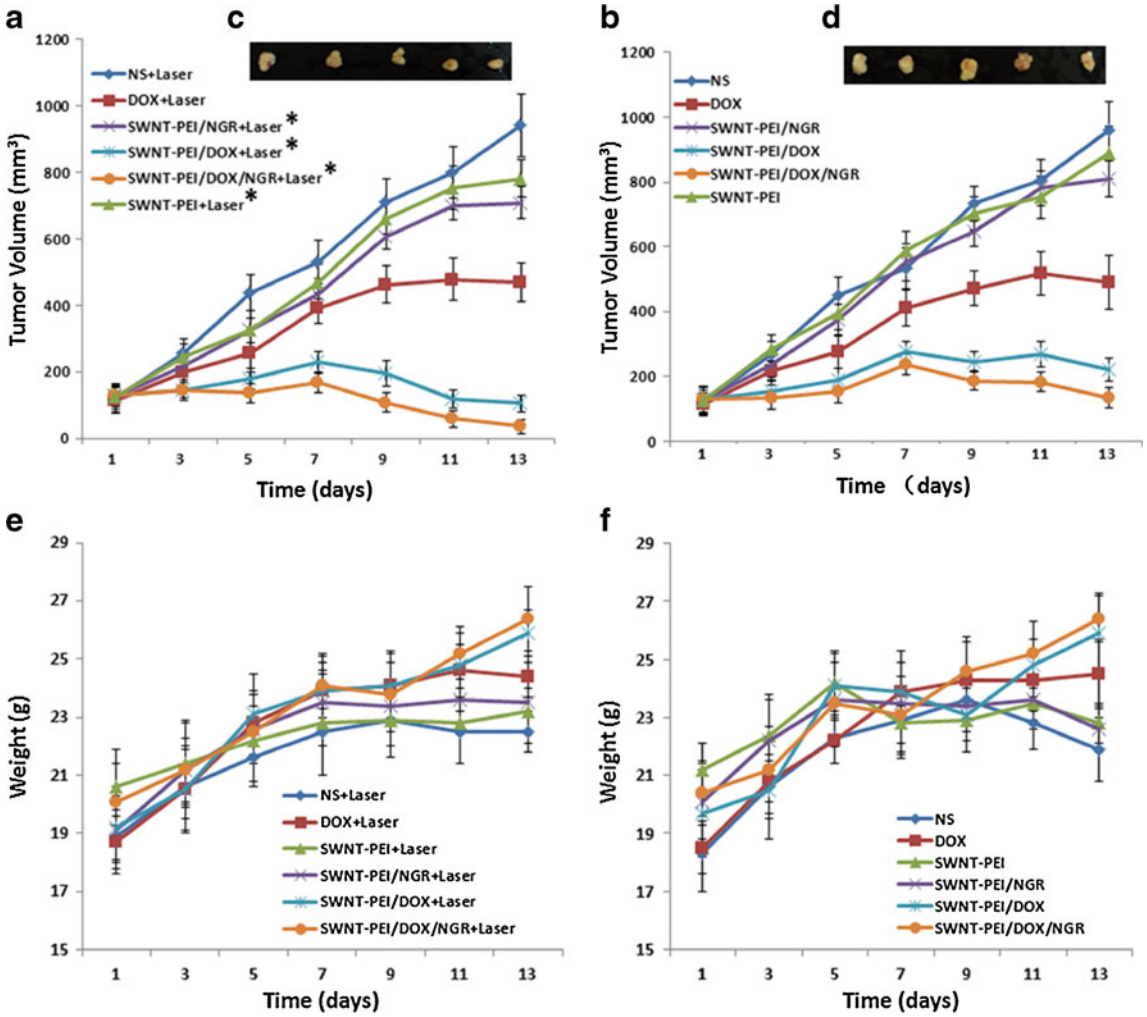

Fig. 9 MCF-7 tumor-bearing nude mice model with or without NIR laser treatment: Average tumor size in nude mice models under treatment with (**a**) or without (**b**) 808 nm NIR laser irradiation *in vivo*; image of dissected tumors of SWNT-PEI/DOX/NGR with (**c**) or without (**d**) laser irradiation; mean body weight of nude mice in different groups with (**e**) or without (**f**) laser irradiation. The SWNT-PEI/DOX/NGR + Laser group showed significant ($P < 0.05$) suppression of tumor growth compared with the other experimental groups with laser irradiation ($n = 5$), and each laser irradiation group containing SWNT shows significant (*$P < 0.05$) suppression of tumor growth compared with the group without laser irradiation treatment, respectively. (Mean + SD, $n = 5$).

delivery system to mice. All these results indicated that the SWNT-PEI vector can delivery chemotherapy drugs with NIR-/pH-responsive, sustained-release, and enhance tumor-targeting effects *in vitro* and *in vivo*.

Histological Analysis

In this study, histological analysis was performed in the major organs including heart, liver, spleen, lung, kidney and tumor with or without NIR laser irradiation in nude mice (Fig. 10). It is well known that the cytotoxicity of SWNTs is a concern for their *in vivo* applications (12–14,38,39). Physicochemical properties of SWNTs such as shape, diameter, conductance and surface chemistry of SWNTs gained during manufacturing processes play a key role in their toxicity (40). A number of studies showed that SWNTs with carefully designed biocompatible coatings are harmless to cells *in vitro* and *in vivo* within tested dose ranges (41,42).

Herein, the results of nude mice tissues in all groups containing SWNTs showed no significant toxicity among the major organs compared with control group (NS group), but clear differences in tumor histology were detected. Tumor cells were more heterogenous with cell necrosis, cell lysis and cell fragment to a certain extent occurred in H&E staining sections from DOX, SWNT-PEI/DOX and SWNT-PEI/DOX/NGR groups. No significant morphological change was found in SWNT-PEI, SWNT-PEI/NGR and NS groups, respectively. However, regarding the laser groups, no significant change was found in NS + laser group, and the number of cells in SWNT-PEI and SWNT-PEI/NGR groups was decreased and some nuclei condensed, while the cells

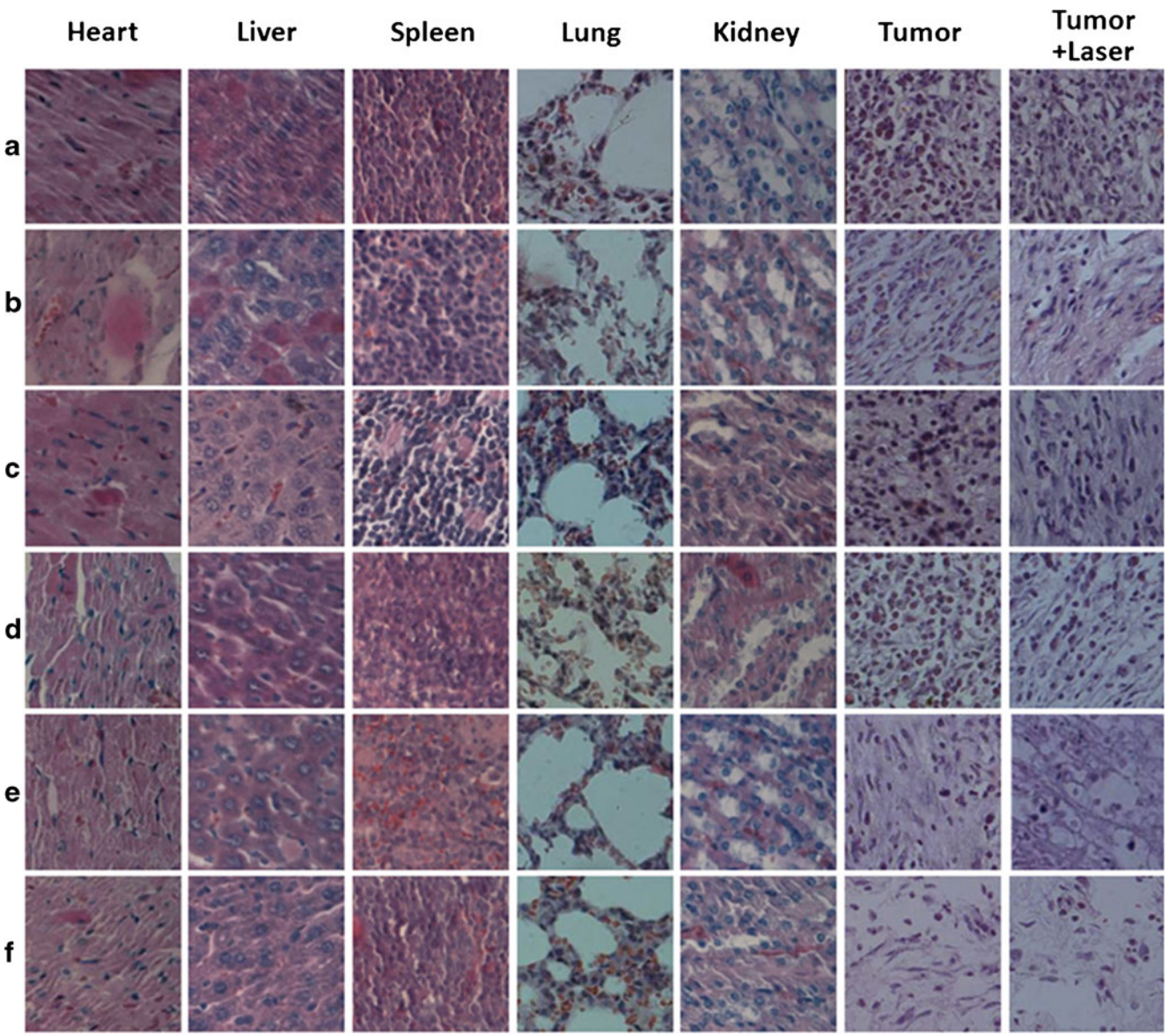

Fig. 10 Histologic assessments of major organs and tumor tissues with H&E staining in nude mice (200×). (**a**) NS, (**b**) DOX, (**c**) SWNT-PEI, (**d**) SWNT-PEI/NGR, (**e**) SWNT-PEI/DOX, (**f**) SWNT-PEI/DOX/NGR. (400×).

construction in SWNT-PEI/DOX and SWNT-PEI/DOX/NGR groups was friable, and the nuclear membrane appeared unsmooth, indicating that chemo-photothermal therapy obviously changed the morphology of tumor tissues.

CONCLUSIONS

In conclusion, a SWNT-PEI/DOX/NGR intelligent delivery system was successfully developed, which showed the characteristics of NIR-/pH-responsiveness, sustained-release, and tumor-targeting. DOX delivered by SWNT-PEI/DOX/NGR presented significant tumor growth inhibition *in vitro* and *in vivo*, demonstrating that the intelligent delivery system has potential to be applied in chemo-photothermal therapy.

ACKNOWLEDGMENTS AND DISCLOSURES

This work was supported by the National Science Foundation of China under grant NO. 81273451 and 30973660.

REFERENCES

1. Sun CY, Qin C, Wang XL, Yang GS, Shao KZ, Lan YQ, *et al.* Zeolitic Imidazolate framework-8 as efficient pH-sensitive drug delivery vehicle. Dalton Trans. 2012;41:6906–9.

2. Nguyen HN, Wey SP, Juang JH, Sonaje K, Ho YC, Chuang EY, *et al.* The glucose-lowering potential of exendin-4 orally delivered via a pH-sensitive nanoparticle vehicle and effects on subsequent insulin secretion in vivo. Biomaterials. 2011;32:2673–82.
3. Huynh CT, Nguyen MK, Lee DS. Biodegradable pH/temperature-sensitive oligo(beta-amino ester urethane) hydrogels for controlled release of doxorubicin. Acta Biomater. 2011;7:3123–30.
4. You J, Zhang R, Zhang G, Zhong M, Liu Y, Van Pelt CS, *et al.* Photothermal-chemotherapy with doxorubicin-loaded hollow gold nanospheres: a platform for near-infrared light-trigged drug release. J Control Release. 2012;158:319–28.
5. Wu H, Zhu L, Torchilin VP. pH-sensitive poly(histidine)-PEG/DSPE-PEG co-polymer micelles for cytosolic drug delivery. Biomaterials. 2012;34:1213–22.
6. Cui ZK, Bouisse A, Cottenye N, Lafleur M. Formation of pH-sensitive cationic liposomes from a binary mixture of monoalkylated primary amine and cholesterol. Langmuir. 2012;28:13668–74.
7. Sun L, Ma X, Dong CM, Zhu B, Zhu X. NIR-responsive and lectin-binding doxorubicin-loaded nanomedicine from Janus-type dendritic PAMAM Amphiphiles. Biomacromolecules. 2012;13:3581–91.
8. Stubbs M, McSheehy PM, Griffiths JR, Bashford CL. Causes and consequences of tumour acidity and implications for treatment. Mol Med Today. 2000;6:15–9.
9. Fang C, Kievit FM, Cho YC, Mok H, Press OW, Zhang M. Effect of cationic side-chains on intracellular delivery and cytotoxicity of pH sensitive polymer-doxorubicin nanocarriers. Nanoscale. 2012;4:7012–20.
10. Kim D, Lee ES, Park K, Kwon IC, Bae YH. Doxorubicin loaded pH-sensitive micelle: antitumoral efficacy against ovarian A2780/DOXR tumor. Pharm Res. 2008;25:2074–82.
11. Moghimi SM, Hunter AC, Murray JC. Long-circulating and target-specific nanoparticles: theory to practice. Pharmacol Rev. 2001;53:283–318.
12. Gottipati MK, Kalinina I, Bekyarova E, Haddon RC, Parpura V. Chemically functionalized water-soluble single-walled carbon nanotubes modulate morpho-functional characteristics of astrocytes. Nano Lett. 2012;12:4742–7.
13. Bayazit MK, Clarke LS, Coleman KS, Clarke N. Pyridine-functionalized single-walled carbon nanotubes as gelators for poly(acrylic acid) hydrogels. J Am Chem Soc. 2010;132:15814–9.
14. Chen J, Chen S, Zhao X, Kuznetsova LV, Wong SS, Ojima I. Functionalized single-walled carbon nanotubes as rationally designed vehicles for tumor-targeted drug delivery. J Am Chem Soc. 2008;130:16778–85.
15. Zhou F, Xing D, Ou Z, Wu B, Resasco DE, Chen WR. Cancer photothermal therapy in the near-infrared region by using single-walled carbon nanotubes. J Biomed Opt. 2009;14:021009.
16. Zhengand X, Zhou F. Noncovalent functionalization of single-walled carbon nanotubes by indocyanine green: potential nanocomplexes for photothermal therapy. J Xray Sci Technol. 2011;19:275–84.
17. Kam NW, O'Connell M, Wisdom JA, Dai H. Carbon nanotubes as multifunctional biological transporters and near-infrared agents for selective cancer cell destruction. Proc Natl Acad Sci U S A. 2005;102:11600–5.
18. Wang L, Zhang M, Zhang N, Shi J, Zhang H, Li M, *et al.* Synergistic enhancement of cancer therapy using a combination of docetaxel and photothermal ablation induced by single-walled carbon nanotubes. Int J Nanomedicine. 2011;6:2641–52.
19. Wang L, Shi J, Zhang H, Li H, Gao Y, Wang Z, *et al.* Synergistic anticancer effect of RNAi and photothermal therapy mediated by functionalized single-walled carbon nanotubes. Biomaterials. 2013;34:262–74.
20. Lu J, Jeon E, Lee BS, Onyuksel H, Wang ZJ. Targeted drug delivery crossing cytoplasmic membranes of intended cells via ligand-grafted sterically stabilized liposomes. J Control Release. 2006;110:505–13.
21. Pasqualini R, Koivunen E, Kain R, Lahdenranta J, Sakamoto M, Stryhn A, *et al.* Aminopeptidase N is a receptor for tumor-homing peptides and a target for inhibiting angiogenesis. Cancer Res. 2000;60:722–7.
22. Corti A, Curnis F, Arap W, Pasqualini R. The neovasculature homing motif NGR: more than meets the eye. Blood. 2008;112:2628–35.
23. Fukasawa K, Fujii H, Saitoh Y, Koizumi K, Aozuka Y, Sekine K, *et al.* Aminopeptidase N (APN/CD13) is selectively expressed in vascular endothelial cells and plays multiple roles in angiogenesis. Cancer Lett. 2006;243:135–43.
24. Min M, Wang X, Yang Y, Liu Z, Zhou Z, Zhu M, *et al.* Fabrication of micro-nano structure nanofibers by solvent etching. J Nanosci Nanotechnol. 2011;11:6919–25.
25. Chaban VV, Savchenko TI, Kovalenko SM, Prezhdo OV. Heat-driven release of a drug molecule from carbon nanotubes: a molecular dynamics study. J Phys Chem B. 2010;114:13481–6.
26. Wang X, Wang C, Cheng L, Lee ST, Liu Z. Noble metal coated single-walled carbon nanotubes for applications in surface enhanced Raman scattering imaging and photothermal therapy. J Am Chem Soc. 2012;134:7414–22.
27. Zhou F, Wu S, Wu B, Chen WR, Xing D. Mitochondria-targeting single-walled carbon nanotubes for cancer photothermal therapy. Small. 2011;7:2727–35.
28. Kosuge H, Sherlock SP, Kitagawa T, Dash R, Robinson JT, Dai H, *et al.* Near infrared imaging and photothermal ablation of vascular inflammation using single-walled carbon nanotubes. J Am Heart Assoc. 2012;1:e002568.
29. Xiong W, Wang W, Wang Y, Zhao Y, Chen H, Xu H, *et al.* Dual temperature/pH-sensitive drug delivery of poly(N-isopropylacrylamide-co-acrylic acid) nanogels conjugated with doxorubicin for potential application in tumor hyperthermia therapy. Colloids Surf B Biointerfaces. 2011;84:447–53.
30. Zandberg WF, Bakhtiari AB, Erno Z, Hsiao D, Gates BD, Claydon T, *et al.* Photothermal release of small molecules from gold nanoparticles in live cells. Nanomedicine. 2012;8:908–15.
31. Sherlock SP, Tabakman SM, Xie L, Dai H. Photothermally enhanced drug delivery by ultrasmall multifunctional FeCo/graphitic shell nanocrystals. ACS Nano. 2011;5:1505–12.
32. Ma X, Zhang L, Wang L, Xue X, Sun JH, Wu Y, *et al.* Single-walled carbon nanotubes alter cytochrome C electron transfer and modulate mitochondrial function. ACS Nano. 2012;6:10486–96.
33. Liu X, Tao H, Yang K, Zhang S, Lee ST, Liu Z. Optimization of surface chemistry on single-walled carbon nanotubes for in vivo photothermal ablation of tumors. Biomaterials. 2011;32:144–51.
34. Liu R, He B, Li D, Lai Y, Chang J, Tang JZ, *et al.* Effects of pH-sensitive chain length on release of doxorubicin from mPEG-b-PH-b-PLLA nanoparticles. Int J Nanomedicine. 2012;7:4433–46.
35. Dreischaluck J, Schwoppe C, Spieker T, Kessler T, Tiemann K, Liersch R, *et al.* Vascular infarction by subcutaneous application of tissue factor targeted to tumor vessels with NGR-peptides: activity and toxicity profile. Int J Oncol. 2010;37:1389–97.
36. Sheihet L, Garbuzenko OB, Bushman J, Gounder MK, Minko T, Kohn J. Paclitaxel in tyrosine-derived nanospheres as a potential anti-cancer agent: in vivo evaluation of toxicity and efficacy in comparison with paclitaxel in Cremophor. Eur J Pharm Sci. 2012;45:320–9.
37. Synold TW, Xi B, Wu J, Yen Y, Li BC, Yang F, *et al.* Single-dose pharmacokinetic and toxicity analysis of pyrrole-imidazole polyamides in mice. Cancer Chemother Pharmacol. 2012;70:617–25.

38. Sacharand S, Saxena RK. Cytotoxic effect of poly-dispersed single walled carbon nanotubes on erythrocytes in vitro and in vivo. PLoS One. 2011;6:e22032.
39. Zhang Y, Deng J, Guo F, Li C, Zou Z, Xi W, et al. Functionalized single-walled carbon nanotubes cause reversible acute lung injury and induce fibrosis in mice. J Mol Med (Berl). 2013;91:117–28.
40. Park EJ, Roh J, Kim SN, Kang MS, Lee BS, Kim Y, *et al.* Biological toxicity and inflammatory response of semi-single-walled carbon nanotubes. PLoS One. 2011;6:e25892.
41. Doan BT, Seguin J, Breton M, Le Beherec R, Bessodes M, Rodriguez-Manzo JA, *et al.* Functionalized single-walled carbon nanotubes containing traces of iron as new negative MRI contrast agents for in vivo imaging. Contrast Media Mol Imaging. 2012; 7:153–9.
42. Kawaguchi M, Ohno J, Irie A, Fukushima T, Yamazaki J, Nakashima N. Dispersion stability and exothermic properties of DNA-functionalized single-walled carbon nanotubes. Int J Nanomedicine. 2011;6:729–36.